Cell Reports
Article

TET1 Suppresses Cancer Invasion by Activating the Tissue Inhibitors of Metalloproteinases

Chih-Hung Hsu,[1,11,13] Kai-Lin Peng,[1,2,11] Ming-Lun Kang,[1,12] Yi-Ren Chen,[3,12] Yu-Chih Yang,[3] Chin-Hsien Tsai,[3,4] Chi-Shuen Chu,[1,5] Yung-Ming Jeng,[6] Yen-Ting Chen,[1,5] Feng-Mao Lin,[7] Hsien-Da Huang,[7] Yun-Yuh Lu,[1] Yu-Ching Teng,[1,2] Shinn-Tsuen Lin,[8] Ruo-Kai Lin,[1,14] Fan-Mei Tang,[9] Sung-Bau Lee,[1,15] Huan Ming Hsu,[10] Jyh-Cherng Yu,[10,*] Pei-Wen Hsiao,[3,*] and Li-Jung Juan[1,2,5,*]

[1]Genomics Research Center, Academia Sinica, Taipei 115, Taiwan, ROC
[2]Institute of Biochemistry and Molecular Biology, National Yang-Ming University, Taipei 112, Taiwan, ROC
[3]Agricultural Biotechnology Research Center, Academia Sinica, Taipei 115, Taiwan, ROC
[4]Institute of Biochemical Sciences, National Taiwan University, Taipei 106, Taiwan, ROC
[5]Institute of Molecular Medicine, College of Medicine, National Taiwan University, Taipei 100, Taiwan, ROC
[6]Graduate Institute of Pathology, National Taiwan University, Taipei 100, Taiwan, ROC
[7]Department of Biological Science and Technology, Institute of Bioinformatics and Systems Biology, National Chiao Tung University, Hsinchu 300, Taiwan, ROC
[8]R&D department, GeneTex Asia Ltd, Hsinchu 300, Taiwan, ROC
[9]Institute of Biomedical Sciences, Academia Sinica, Taipei 115, Taiwan, ROC
[10]Division of General Surgery, Department of Surgery, Tri-Service General Hospital, National Defense Medical Center, Taipei 114, Taiwan, ROC
[11]These authors contributed equally to this work
[12]These authors contributed equally to this work
[13]Present address: Division of Newborn Medicine, Children's Hospital Boston, Harvard Medical School, Boston, MA 02115, USA
[14]Present address: Graduate Institute of Pharmacology, Taipei Medical University, Taipei 110, Taiwan, ROC
[15]Present address: Biotech Research and Innovation Centre (BRIC), University of Copenhagen, DK2200 Copenhagen, Denmark
*Correspondence: doc20106@ndmctsgh.edu.tw (J.-C.Y.), pwhsiao@gate.sinica.edu.tw (P.-W.H.), ljjuan@gate.sinica.edu.tw (L.-J.J.)
http://dx.doi.org/10.1016/j.celrep.2012.08.030

SUMMARY

Tumor suppressor gene silencing through cytosine methylation contributes to cancer formation. Whether DNA demethylation enzymes counteract this oncogenic effect is unknown. Here, we show that TET1, a dioxygenase involved in cytosine demethylation, is downregulated in prostate and breast cancer tissues. TET1 depletion facilitates cell invasion, tumor growth, and cancer metastasis in prostate xenograft models and correlates with poor survival rates in breast cancer patients. Consistently, enforced expression of TET1 reduces cell invasion and breast xenograft tumor formation. Mechanistically, TET1 suppresses cell invasion through its dioxygenase and DNA binding activities. Furthermore, TET1 maintains the expression of tissue inhibitors of metalloproteinase (TIMP) family proteins 2 and 3 by inhibiting their DNA methylation. Concurrent low expression of *TET1* and *TIMP2* or *TIMP3* correlates with advanced node status in clinical samples. Together, these results illustrate a mechanism by which TET1 suppresses tumor development and invasion partly through downregulation of critical gene methylation.

INTRODUCTION

Tumor growth and cancer formation is controlled by both genetic and epigenetic events (Dawson and Kouzarides, 2012; You and Jones, 2012). Cancer epigenetic events include aberrant DNA methylation such as localized CpG island hypermethylation that leads to inactivation of specific tumor-suppressor genes (Kulis and Esteller, 2010; Taberlay and Jones, 2011). While DNA methyltransferases have been demonstrated to be oncogenic by silencing tumor-suppressor genes via cytosine methylation, whether enzymes with opposing function protect cells from becoming malignant remains elusive.

The ten eleven translocation (TET) family of proteins, TET1, TET2, and TET3, were discovered on the basis of *TET1* fusion to the *mixed lineage leukemia* gene in acute myeloid leukemia (Lorsbach et al., 2003; Ono et al., 2002). In 2009, TET1 was found to be a dioxygenase that converts 5-methylcytosine (5mC) to 5-hydroxymethylcytosine (5hmC) (Tahiliani et al., 2009). The same activity of TET1 and its role in mouse embryonic stem cells was identified by another independent group (Ito et al., 2010). Moreover, TET proteins were demonstrated to be capable of further converting 5hmC to 5-formylcytosine and 5-carboxylcytosine, which can be excised by thymine DNA glycosylase (He et al., 2011; Ito et al., 2010; Ito et al., 2011; Tahiliani et al., 2009; Wu and Zhang, 2010). Functions of TET proteins are believed to rely on the CXXC domain for DNA binding in TET1 and on the double-stranded β helix domain for the 2-oxoglutarate- and Fe(II)-dependent oxygenase activity (Wu and Zhang, 2011a; Xu et al., 2011b). Importantly, not only are TET proteins potentially involved in the active DNA demethylation process, they have also been shown to prevent DNA methylation by physically binding to DNA (Wu and Zhang, 2011a). Whether TET proteins play any role in cancer formation remains an intriguing question. It has been revealed that the catalytic TET2 mutations with decreased 5hmC are associated with myeloid cancers (Ko et al., 2010). Loss of TET1 and 5hmC in

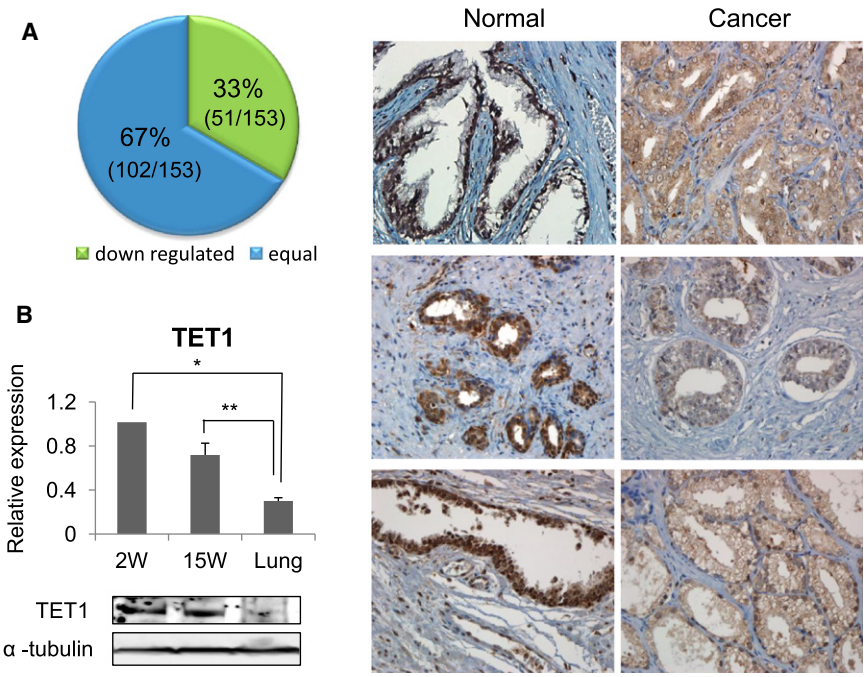

Figure 1. TET1 Is Decreased in Human Prostate Cancer Tissues and Implanted Prostate Cancer Cells Metastasized from Mouse Prostate to Lung

(A) IHC detection of TET1 protein in normal and cancerous human prostate tissues. Shown in right are three representative examples of normal adjacent tissues and tumor sections. Original magnification, ×200 (normal), ×400 (cancer).

(B) TET1 expression inversely correlates with prostate cancer progression. Relative TET1 mRNA and protein levels in human prostate cancer 22Rv1 cells from mouse prostate at week 2 (2W) or 15 (15W), or from lung at week 15 (lung) after implantation of 22Rv1 into the prostate of nude mice are shown as mean ± SD from triplicate experiments for RT-PCR. p values were measured by Student's t test. *$p < 0.05$; **$p < 0.01$.

solid tumors is recently reported as well (Haffner et al., 2011; Jin et al., 2011; Kudo et al., 2012; Yang et al., 2012). However, to date, the underlying mechanism and target genes involved in the TET family of proteins' function in cancer are unknown.

Cell invasion is one of the pivotal steps in both primary tumor growth and metastasis initiation (Deryugina and Quigley, 2006; Friedl and Alexander, 2011; Hojilla et al., 2008; Hua et al., 2011). The matrix metalloproteinase (MMP) family of proteins and their endogenous regulators, tissue inhibitors of metalloproteinases (TIMPs), are key players in the modulation of cell invasion and epithelial-mesenchymal transition (Bourboulia and Stetler-Stevenson, 2010; Kessenbrock et al., 2010; Murphy, 2011). For example, MMP2 and MMP9 stimulate cell invasion by inducing basement membrane damage and focal degradation of type IV collagen and laminin (Zeng et al., 1999). Although it is not completely understood, one of the major functions of TIMP proteins is to inhibit the activities of MMPs by binding to the active site of MMPs or sequestering the pro-MMP zymogens (Clark et al., 2008; Murphy, 2011). Interestingly, the expression of some of the *TIMP* genes is known to be regulated by DNA methylation (Chernov et al., 2009).

In the current study, we demonstrate the suppressive role of TET1 in both prostate and breast cancer invasion by using cell-based assays, xenograft models, and human clinical tissue samples. Furthermore, we show that the MMP inhibitors TIMP2 and TIMP3 are pivotal TET1 downstream effectors responsible for TET1-mediated invasion suppression.

RESULTS AND DISCUSSION

TET1 Expression Is Downregulated in Prostate Cancer

Given the established role of DNA methylation in cancer, we investigated whether TET1, a protein recently shown to play a role in regulating DNA demethylation, is involved in tumor development. In an examination of *TET1* expression in different human tissues, we found that *TET1* mRNA level was enriched in prostate, breast, and ovary tissues as compared to lung, liver, and colon tissues (data not shown), indicating that TET1 might have important functions in these endocrine-related tissues. We then hypothesized that, if TET1 serves as a tumor suppressor, loss of TET1 might play a role in the development of tumors derived from these TET1-rich tissues. To test this hypothesis, we first investigated prostate cancer. Immunohistochemical staining demonstrated that 33% of 153 prostate cancer patients showed reduced TET1 expression in cancerous cells as compared to non-neoplastic glands, while 67% had equal TET1 levels (Figure 1A). Note that the samples were diagnosed as prostate cancer cells via H&E staining and stained with rabbit IgG as a negative control (data not shown). Furthermore, we found that TET1 downregulation was likely involved in cancer metastasis, as demonstrated in the following experiments. To evaluate the role of specific genes in cancer metastasis, we previously developed a mouse system (Tsai et al., 2009) in which highly invasive and puromycin-resistant human prostate cancer 22Rv1 cells tagged with a luciferase reporter gene were orthotopically implanted into the prostate of nude mice. At different times after implantation, cells from prostate or lung tissue were evaluated for the expression of luciferase, followed by isolation with puromycin selection. In this way, the metastasis of implanted cells can be analyzed. Using this animal model, we demonstrated that both the mRNA and protein levels of *TET1* were dramatically reduced during the metastasis of transplanted 22Rv1 cells from prostate to lung (Figure 1B), indicating that TET1 expression is negatively associated with the progression of prostate cancer metastasis.

TET1 Suppresses Prostate Cancer Invasion and Metastasis

To evaluate whether TET1 indeed plays a role in the metastasis process, we generated a TET1 knockdown shRNA (designated

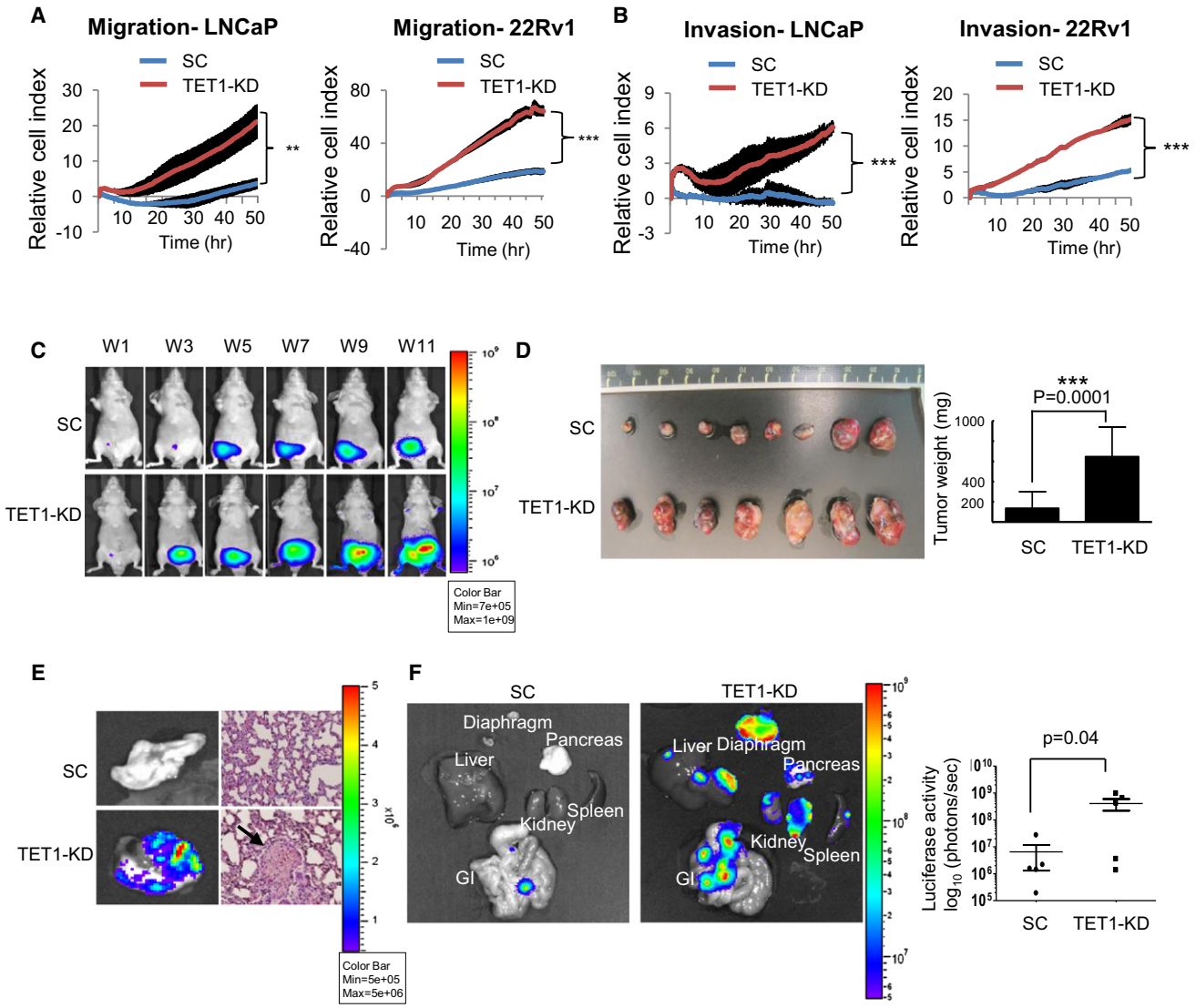

Figure 2. TET1 Depletion Stimulates Prostate Cancer Invasion and Metastasis In Vitro and In Vivo

(A and B) TET1 knockdown promotes migration (A) and invasion (B) of prostate cancer cells LNCaP and 22Rv1. The migrating or invading cells with scramble shRNA (SC) or *TET1* shRNA (TET1-KD) were analyzed by Roche xCELLigence, and the data are shown as cell index curves with mean ± SD from triplicate experiments.

(C–E) TET1 knockdown facilitates the tumorigenesis (C and D) and metastasis (E) of LNCaP-derived prostate cancer xenografts in nude mice.

(C) The luciferase images of the cancer cells in representative mice taken at the indicated time. A total of eight and seven mice were analyzed in the control and TET1-KD groups, respectively.

(D) Left: photograph of dissected tumors from mice taken at week 12 after implantation. Right: relative tumor weight.

(E) Left: bioluminescence images of the host lungs from mice taken at week 12 after implantation. Right: microscopic examination with H&E staining for the verification of in situ pulmonary metastasis (arrow).

(F) TET1 depletion facilitates metastasis of 22Rv1-derived prostate cancer xenografts in nude mice. Left: ex vivo image of the peritoneal organs isolated from each group of mice at endpoint. Right: quantification of the bioluminescent image on the left.

p values were measured by repeated-measure ANOVA in (A) and (B) and by Student's t test in (D) and (F). **$p < 0.01$; ***$p < 0.001$.

KD1, used throughout the study) and confirmed its efficiency in depleting *TET1* mRNA (Figure S1A) and protein (Figure S1B) from cells. The *TET1* shRNA also increased and decreased the levels of 5mC and 5hmC, respectively (Figure S1C). Consistent with a potential role of TET1 in suppressing cancer metastasis, knocking down *TET1* facilitated migration and invasion of both low (LNCaP) and high (22Rv1) invasive prostate cancer cells in an in vitro cell-based assay (Figures 2A, 2B and S2). Interestingly, we noted that TET1 depletion slightly increased prostate cancer cell proliferation (Figure S3). Nevertheless, the fold increase of migration was more than the fold increase of proliferation in both LNCaP and 22Rv1 cells depleted of TET1 (compare

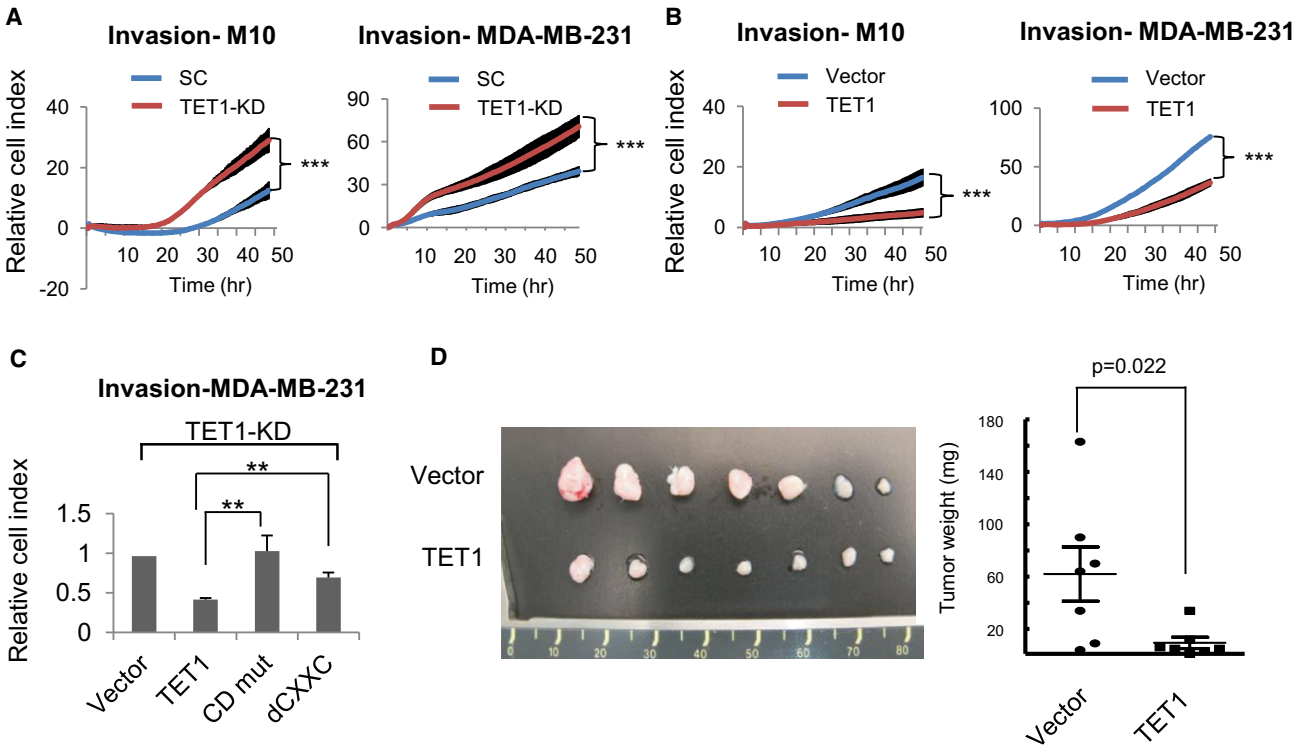

Figure 3. TET1 Inhibits Breast Cancer Cell Invasion and Tumor Formation

(A) TET1 knockdown stimulates cell invasion. The invading M10 (left) or MDA-MB-231 (right) cells with or without *TET1* shRNA were analyzed by Roche xCELLigence, and the data are shown as cell index curves with mean ± SD from triplicate experiments.

(B) TET1 overexpression represses cell invasion. The invading M10 or MDA-MB-231 cells with or without expression of Flag-tagged TET1 were analyzed for invasion ability as in (A).

(C) TET1 suppression of cell invasion requires intact catalytic and CXXC domains. MDA-MB-231 cells expressing *TET1* shRNA were transfected with vector alone, WT TET1 (TET1), catalytic mutant (CD mut), or CXXC-deleted mutant (dCXXC), followed by cell invasion analysis at 24 hr by Roche xCELLigence.

(D) Inducible expression of TET1 inhibits breast xenograft tumor formation. Left: photograph of mammary tumors from 4T1-vector and 4T1-TET1 cells, dissected at week 3 after implantation. Right: quantification of the bioluminescent image on the left.

Data from (A) to (C) are shown as mean ± SD. p values were measured by repeated-measure ANOVA in (A) and (B), and by Student's t test in (C) and (D). $^{**}p < 0.01$; $^{***}p < 0.001$.

Figure 2A with Figure S3). Therefore, it is unlikely that the observed increase in migration and invasion of TET1-deficient cells was simply due to the enhanced cell proliferation.

To substantiate the in vitro observations in vivo, we analyzed whether depletion of TET1 promotes prostate cancer cell metastasis in mice. To this end, control and TET1-depleted prostate cancer cells tagged with luciferase were injected into the prostate of nude mice, followed by analysis of proliferation and metastasis of the injected cells at week 12 after implantation. The results demonstrated that TET1-depleted LNCaP (Figures 2C and 2D) or 22Rv1 cells (Figures S4A and S4B) formed larger tumors. Xenograft experiments further demonstrated that elimination of TET1 facilitated metastasis of transplanted 22Rv1 (Figure S4C) or LNCaP (Figures 2E, S4D, and S4E) cells from prostate to lung in vivo, as evidenced by the metastasis microscopically observed in lung tissue. Increased metastasis of TET1-depleted 22Rv1 cells to organs other than the lung was also observed (Figure 2F). Collectively, the results above indicate that TET1 most likely inhibits prostate cancer metastasis and the underlying mechanism may involve TET1-mediated downregulation of cell migration and invasion.

TET1 Inhibits Breast Cancer Cell Invasion and Xenograft Tumor Growth

Subsequently, we asked whether the role of TET1 in suppressing prostate cancer metastasis can be extended to breast cancer. To this end, we eliminated TET1 from normal (M10) and cancerous (MDA-MB-231) breast cells (Figures S1A and S1C) and analyzed its effect on cell invasion. The results shown in Figure 3A and Figure S5A demonstrated that TET1 depletion by *TET1* shRNA KD1 increased the cell-invasion capacity. Using another independent *TET1* shRNA, KD2, we observed a similar effect in M10 cells (Figures S5B and S5C). Consistently, ectopic expression of TET1 reduced cell invasion (Figure 3B). Note that TET1 depletion decreased the proliferation of both M10 and MDA-MB-231 cells (Figure S5D), ruling out the possibility that the increased invasion by *TET1* shRNA was due to enhanced cell proliferation. To evaluate whether the invasion suppression capacity of TET1 requires its enzymatic or CpG binding activity, we generated a TET1 mutant with amino acid substitutions in the catalytic domain (CD mut) or a deletion in the CpG binding domain CXXC (dCXXC mut) and expressed the mutants and wild-type TET1, respectively (Figure S6A). We then used a dot

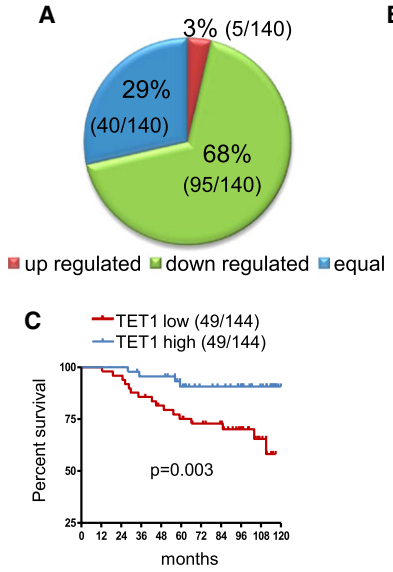

B

Clinical pathological characteristics of breast cancer patients with associated TET1 expression

Characteristics	TET1 high (49/144)	TET1 low (49/144)	*P* value
Age	51.89 ± 11.96	51.00 ± 13.75	0.74[1]
Tumor size (cm)	1.80 ± 0.85	2.48 ± 1.33	0.004[1]
Stage (no. of patients)			0.004[2]
is-I	29 (59%)	15 (31%)	
II-IV	20 (41%)	34 (69%)	
Tumor status (no. of patients)			0.03[2]
Tis-T1	37 (76%)	27 (55%)	
T2-T4	12 (24%)	22 (45%)	
Node status (no. of patients)			0.007[2]
N0	36 (73%)	23 (47%)	
N1-N2	13 (27%)	26 (53%)	

[1]p value was measured with student's t test.
[2]significance of association was determined using a χ^2 test.

Figure 4. TET1 Downregulation Correlates with Advanced Stage and Poor Survival in Breast Cancer Patients

(A) TET1 is downregulated in the majority of the breast cancer tissues. The mRNA level of *TET1* in human cancerous breast tissue specimens or adjacent normal tissues was analyzed and normalized to actin. In 140 sample pairs, 95 (68%) have decreased levels of *TET1* mRNA in cancer tissues (green), 40 (29%) show equal *TET1* mRNA levels (blue), and 5 (3%) exhibit higher levels of *TET1* mRNA in cancerous tissues (red).

(B) TET1 downregulation positively correlates with larger tumor and advanced stage of breast cancer. Patients were grouped into tertiles based on *TET1* expression levels. 49 patients with the lowest or highest expression levels of TET1 in the cancer tissues from 144 breast cancer patients, overlapping with 140 patients in (A), were analyzed in terms of the relationship between TET1 expression and clinical parameters including age, tumor size, cancer stage, tumor status, and node status. Stage was determined according to the AJCC system. p values were measured according to methods indicated at the bottom of the panel.**p < 0.01; ***p < 0.001.

(C) TET1 expression inversely correlates with breast cancer patient survival. The same sets of breast cancer patients as in (B) were analyzed. The survival rates of breast cancer patients were estimated by Kaplan-Meier analysis. Log-rank test was used to compare the survival rates between the upper and lower tertile of patients on the basis of *TET1* expression level.

blot assay to confirm that the CD mut did lose the ability to erase the cellular 5mC signal, while the dCXXC mut still retained the ability (Figure S6B). The phenotype of the dCXXC mut is consistent with that observed in a previous study (Frauer et al., 2011). Results shown in Figure 3C demonstrated that re-expression of wild-type (WT) TET1, but not the catalytic mutant, suppressed cell invasion induced by TET1 depletion. In addition, the dCXXC mut failed to repress cell invasion as efficiently as WT TET1 (Figure 3C). These results not only support the specificity of the *TET1* shRNA used but also demonstrate that both the dioxygenase and CpG binding activities are pivotal for TET1 function in invasion suppression. Indeed, TET1 is known to exert its effect through both enzymatic-activity-dependent and -independent manners. It has been reported that, in addition to actively demethylating cytosines, TET1 is able to prevent DNA methylation by physically occupying the unmethylated cytosines (Wu et al., 2011; Xu et al., 2011b). The importance of the catalytic and DNA binding domains in TET1 function was recapitulated in the following experiment. Consistent with the notion that TET1 is most likely a suppressor of breast cancer invasion, consecutive selection in an in vitro invasion assay by six rounds greatly reduced *TET1* mRNA levels in 468-6 cells, the highly invasive fraction of MDA-MB-468 cells (Figure S7A). As expected, re-expression of WT TET1, but not the enzymatic or CXXC mutant, inhibited the cell-invasion capacity of 468-6 cells (Figure S7B). This is consistent with the observation that enzymatic activity and CpG binding capacity are required for TET1-mediated invasion suppression.

To further understand whether the invasion-suppression function of TET1 in breast cancer cells can be observed in vivo, we analyzed tumor development from cells with or without stably inducible expression of TET1. As shown in Figures 3D and S8, mouse mammary carcinoma 4T1 cells with human TET1 expression generated significantly smaller tumors, further confirming the tumor-suppressor role of TET1 in breast cancer.

TET1 Downregulation in Breast Cancer Correlates with Poor Survival Outcomes in Patients

To determine whether the observations above can be verified in human breast cancer tissues, we analyzed *TET1* mRNA levels in 140 breast cancer tissue samples and their normal control tissues by quantitative real-time RT-PCR, using actin as an internal control (Figure S9). Of the 140 pairs of sample tissue, 95 (68%) exhibited lower levels of *TET1* mRNA in cancer tissues as compared with their normal-tissue control counterparts (Figure 4A). Importantly, the lowest tertile of breast cancer patients (n = 49) found to have low expression levels of *TET1* had larger tumors with advanced stage (Figure 4B) and poor survival (Figure 4C) as compared with the highest tertile of patients (n = 49) with high *TET1* expression levels. Similar survival correlation was observed in another independent cohort of 96 breast cancer patients. Moreover, in this second cohort, up to 81% and 79% of patients showed decreased *TET1* expression in cancer tissues when actin and GAPDH, respectively, were used as the internal controls (Figure S10). Together, these results demonstrated that the *TET1* expression level was inversely correlated with breast cancer cell invasion and tumor development, indicating that TET1 might play an important role in suppressing breast cancer progression.

TET1 Promotes the Expression and Function of TIMP2 and TIMP3

Our data indicate that TET1 very likely suppresses the invasion of both prostate and breast cancers. To understand how TET1 is

involved in this process, we performed microarray studies. Comparison of gene expression between control and TET1-depleted M10 cells indicated that 406 genes were differentially expressed (90 upregulated and 316 downregulated) (Figure S11A). We confirmed the fidelity of the microarray results by analyzing representative genes with real time RT-qPCR (Figures S11B–S11D). Given that TET1 suppresses invasion and metastasis, particular attention was paid to the TET1-regulated genes implicated in these processes. Among the 406 potential targets, the *TIMP* family genes *TIMP2* and *TIMP3* are of great interest, not only because of their ability to modulate MMPs (Bourboulia and Stetler-Stevenson, 2010; Kessenbrock et al., 2010; Murphy, 2011) but also because their expression is known to be regulated by DNA methylation (Chernov et al., 2009). The TIMP family comprises the genes *TIMP1*, *TIMP2*, *TIMP3*, and *TIMP4*. We found that TET1 depletion in two types of cancerous prostate cells (LNCaP and 22Rv1) and in normal and cancerous breast cells (M10 and MDA-MB-231, respectively) resulted in downregulation of *TIMP2* and *TIMP3* expression (Figure 5A), indicating that TET1 is a positive regulator of these two genes. mRNA levels of *TIMP2* and *TIMP3* were also found to be diminished in other cells, including human breast cancer cells MCF7 and MDA-MB-468, when TET1 was depleted (Figure S11E). In contrast, the *TIMP1* mRNA level did not seem to be altered by TET1 in a consistent manner: it was slightly upregulated in M10 and only minimally downregulated in MDA-MB-231 when TET1 was knocked down (Figure 5A). *TIMP4* was undetectable in both M10 and MDA-MB-231 cells.

Subsequently, we investigated whether the concurrent expression of TET1 and TIMP2 or TIMP3 observed in cell lines can be recapitulated in vivo. As shown in Figure S12, similar to that of *TET1*, the *TIMP3* mRNA level was also downregulated in implanted 22Rv1 cells metastasized from mouse prostate to lung. Furthermore, breast cancer patients with lower levels of *TET1* expression had significantly lower levels of *TIMP2* and *TIMP3* expression (Figure 5B). Analysis of the same set of breast cancer patients with high expression of *TET1* and *TIMP2* or *TIMP3* or low expression of *TET1* and *TIMP2* or *TIMP3* indicated that concurrent low expression of *TET1* and *TIMP2* or *TIMP3* is correlated with advanced node status (Figure 5C). These studies not only strongly support the hypothesis that TET1 is an upstream activator for the expression of TIMP2 and TIMP3 but also provide the clinical link between reduced expression of TET1, TIMP2, and TIMP3 and breast cancer progression.

Given that one of the pivotal functions of TIMP2 and TIMP3 is to inhibit the activity of MMPs which in general promote cancer invasion and metastasis (Clark et al., 2008; Murphy, 2011), we asked whether TET1 deficiency causes an increase in MMP function. To this end, we performed reverse zymography analysis. As a control, only gelatin, the substrate of MMP2 and MMP9, at the position of TIMP2 (~20 kD) and TIMP3 (~24 kD) remained intact and stained by Coomassie Blue (Figure 5D, lane 1). Upon TET1 depletion, the level of gelatin at these two specific positions was decreased (lane 2), presumably due to the reduced level of TIMP2 and TIMP3 and the increased activity of MMP2 and MMP9. This result strongly suggests that optimal TIMP2 and TIMP3 activities require TET1. Consistently, TET1 knockdown stimulated the total MMP activity, as detected by fluorescence generated by a peptide after cleavage by MMPs (Figure 5E), indicating that TET1 expression is necessary for the inhibition of MMP activity. Together, these experiments uncover an essential role of TET1 in maintaining the expression and function of TIMP2 and TIMP3.

TET1-Mediated Invasion Suppression Requires TIMP2 and TIMP3

To further study whether TIMP2 and TIMP3 directly contribute to TET1-mediated suppression of cell invasion and metastasis, we first ectopically expressed TIMP2 or TIMP3 in TET1-eliminated cells, then performed a cell-invasion assay. As expected, the exogenously expressed TIMP2 or TIMP3 significantly downregulated cell invasion induced by TET1 knockdown (Figure 6A), indicating that expression of TIMP2 or TIMP3 is capable of compensating for the lack of TET1 in invasion suppression. Next we knocked down TIMP2 or TIMP3 to evaluate whether they account for TET1 function in inhibiting invasion. Consistent with previous results (Anania et al., 2011), depletion of TIMP2 or TIMP3 potentiated cell invasion (Figure 6B, bars 1–3). Importantly, TET1 elimination-induced cell invasion (bars 4 and 5) was lost in cells without TIMP2 or TIMP3 (bars 6–9), indicating that TIMP2 and TIMP3 are major factors responsible for TET1 function in breast cancer cell-invasion suppression. Similar results were observed in prostate cancer cells 22Rv1 (Figure S13A). In another prostate cancer cell line, LNCaP, we observed that 50% and 70% of TET1-knockdown-induced cell invasion was lost in cells when TIMP2 or TIMP3, respectively, was depleted (Figure S13B; compare bars 3–6 with bars 1 and 2). Together, these results suggest that TIMP2 and TIMP3 are likely to be the major players responsible for TET1 activity in invasion suppression. In LNCaP, TET1 may function through the collaborated efforts of TIMP2 and TIMP3 as well as other invasion mediators. Given the heterogeneity of cancers and the potential redundancy in the pathways involved in cell invasion, it is not surprising that subtle variation across different cell lines was observed in this case.

TET1 Directly Binds to CpG-Rich Regions of TIMP2 and TIMP3 Genes and Inhibits Their DNA Methylation

After we established that TIMP2 and TIMP3 are important and essential downstream targets of TET1 in invasion suppression, the mechanism by which TET1 activates the expression of *TIMP2* and *TIMP3* genes was further explored. Given that TET1 is known to bind to CpG islands (Ito et al., 2010; Williams et al., 2011; Wu and Zhang, 2011b; Xu et al., 2011b; Zhang et al., 2010) and that both *TIMP2* and *TIMP3*, but not *TIMP1*, genes are enriched in CpG content, we examined the possibility that TET1 may directly regulate *TIMP2* and *TIMP3* expression by binding to their CpG islands. ChIP analysis demonstrated that exogenously expressed Flag-tagged TET1 bound to the CpG-rich regions of *TIMP2* and *TIMP3* genes, but not the upstream distal site (Figures S14A and S14B). Consistently, the endogenous TET1 bound to the *TIMP3* gene through the CpG island, but not other regions of the TIMP3 gene body or the regulatory sequences of *GADD45* (An et al., 2004) (Figure 7A). The endogenous TET1's binding to the *TIMP3* gene was specific, as the ChIP signals within the CpG island were reduced to less than

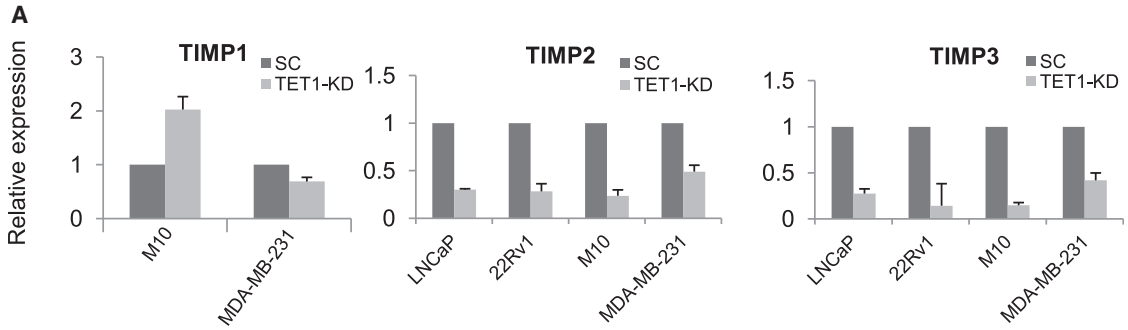

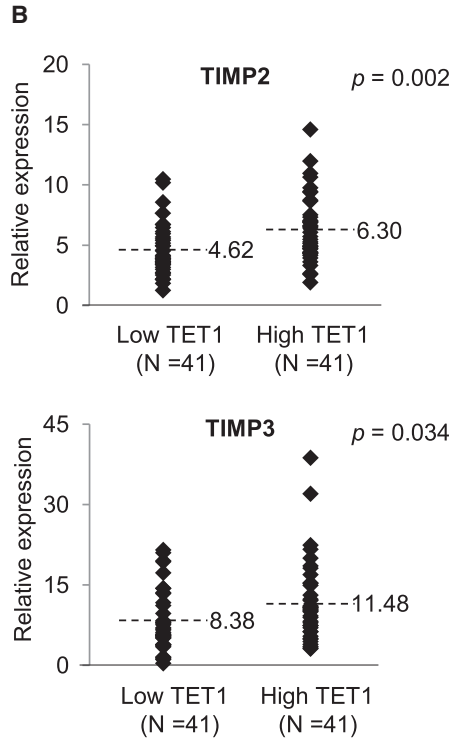

C

Clinical pathological characteristics of breast cancer patients with associated TET1 and TIMP2 expression

Characteristics	TET1 high/ TIMP2 high (20/41)	TET1 low/ TIMP2 low (21/41)	*P* value
Node status (no. of patients)			0.037[1]
N0	15 (75%)	9 (43%)	
N1-N2	5 (25%)	12 (57%)	

Clinical pathological characteristics of breast cancer patients with associated TET1 and TIMP3 expression

Characteristics	TET1 high/ TIMP3 high (20/41)	TET1 low/ TIMP3 low (21/41)	*P* value
Node status (no. of patients)			0.04[1]
N0	14 (70%)	8 (38%)	
N1-N2	6 (30%)	13 (62%)	

[1]significance of association was determined using a χ^2 test.

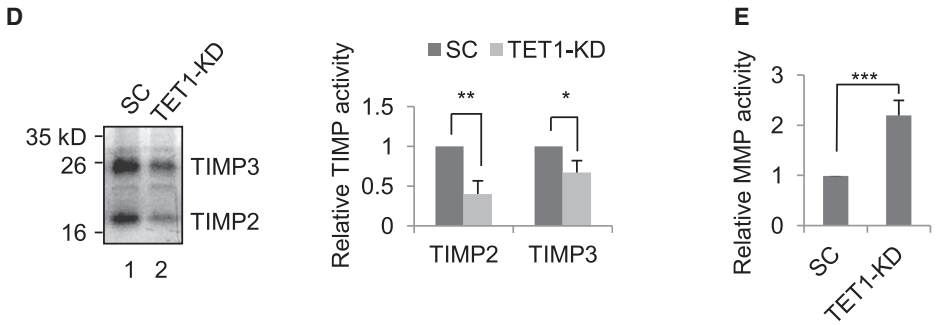

Figure 5. TET1 Is Required for Expression and Function of TIMP2 and TIMP3

(A) Relative mRNA levels of *TIMP1*, *TIMP2*, and *TIMP3* in indicated cells with *TET1* shRNA (TET1-KD) compared to control.

(B) *TIMP2* and *TIMP3* mRNA levels positively correlate with *TET1* expression in clinical breast cancer specimens. Of breast cancer patients, 41 representative patients from each group with the lowest and the highest expression levels of *TET1* in the cancerous tissues (Figure S9) were analyzed for *TIMP2* and *TIMP3* mRNA levels with normalization to actin expression. The mean values are indicated.

(C) Low *TET1* and *TIMP2*, or *TIMP3* levels correlate with advanced node status in clinical breast cancer specimens. The same set of samples as in (B) was analyzed. 41 patients with high or low *TET1* expression were split into two groups with high (n = 20) or low (n = 21) levels of *TIMP2* or *TIMP3* and were analyzed for node status as in Figure 4B.

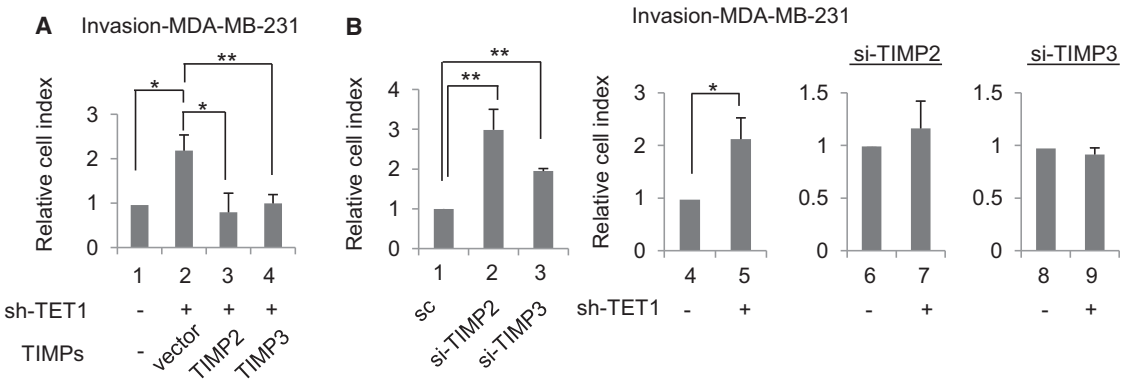

Figure 6. TET1-mediated Invasion Suppression Requires TIMP2 and TIMP3

(A) Exogenous TIMP2 or TIMP3 expression suppresses cell invasion induced by TET1 depletion. MDA-MB-231 cells with *TET1* shRNA were transfected with vector alone or expression plasmid for TIMP2 or TIMP3, followed by cell invasion assay.

(B) TET1 knockdown-induced cell invasion is lost by depletion of TIMP2 and TIMP3. MDA-MB-231 cells with or without *TET1* shRNA were transfected with scramble RNA or siRNA against *TIMP2* or *TIMP3*, followed by cell invasion assay. Data were collected at 42 hr post transfection of siRNA.

Data in (A) and (B) are shown as mean ± SD from triplicate experiments.

50% when the total *TET1* mRNA level was downregulated to around 30% of the initial level by shRNA (Figure 7B). Our result is consistent with previous reports in which TET1 was found to be associated with the gene body, in addition to the gene promoter region and the region around the transcription start site (Williams et al., 2011; Wu et al., 2011). Note that the relative position of the transcription start site of the *TIMP3* gene shown in Figure 7A was defined according to NCBI prediction. Indeed, the structure of *TIMP3* promoter is poorly understood and the position of its transcription start site is controversial. Nevertheless, previous reports have shown that the methylation status of the *TIMP3* gene region found in our study to be bound by TET1 correlates with *TIMP3* gene expression (Bachman et al., 1999). Thus, it is likely that *TIMP3* has a noncanonical promoter that is located downstream of the transcription start site. Together with the data shown in Figure 5, these results suggest that TET1 potentiates the expression of *TIMP2* and *TIMP3* by specifically binding to the CpG-rich sequences of *TIMP2* and *TIMP3* genes.

Given that TET1 is able to convert 5mC to 5hmC, 5-formylcytosine, and 5-carboxycytosine (5caC), which is then removed by thymine DNA glycosylase (TDG)-coupled base excision repair (He et al., 2011; Ito et al., 2011), we analyzed whether TET1's binding to *TIMP2* and *TIMP3* genes alters the methylation status of these two genes. As shown in Figures 7C and S14C, TET1 depletion increased and decreased *TIMP2* and *TIMP3* gene-associated 5mC and 5hmC, respectively. Note that in some TET1-binding regions of these genes, the fold change of TET1-loss-mediated 5mC increase was not exactly comparable to the decrease of 5hmC. We reasoned that 5hmC could be underrepresented because of its conversion to 5caC, which is rapidly removed by TDG. In the regions of amplicons 3 and 4 in M10 cells (Figure 7C), TET1 depletion caused only significant decrease of 5hmC, but not increase of 5mC, suggesting that these DNA regions were decorated with 5hmC instead of 5mC in the presence of TET1 and that these sites were not methylated when TET1 was depleted.

Our results so far strongly suggest that cancer-cell-associated hypermethylation of *TIMP2* and *TIMP3* genes reported previously by others (Bachman et al., 1999; Smith et al., 2008) is most likely due to the loss of TET1 during cancer development. To further test this hypothesis, we treated MDA-MB-231 cells with the DNA methylation inhibitor 5-aza-dC, then *TIMP2* and *TIMP3* mRNA levels were evaluated. Consistent with earlier studies (Anania et al., 2011; Bachman et al., 1999), 5-aza-dC significantly increased *TIMP2* and *TIMP3* expression (Figure 7D). Notably, 5-aza-dC abolished TET1-depletion-mediated suppression of *TIMP2* and *TIMP3* mRNA levels (Figure 7E). Given that 5-aza-dC did not increase TET1 expression in these experiments (data not shown) and that 5-aza-dC is known to reduce the DNA methylation of *TIMP2* and *TIMP3* genes (Bachman et al., 1999; Cameron et al., 1999), these results support the notion that TET1 regulates *TIMP2* and *TIMP3* expression through its controlling of their DNA methylation level. Collectively, these studies indicate that TET1 directly binds to CpG-rich regions of *TIMP2* and *TIMP3* genes and downregulates their DNA methylation. Consequently, loss of TET1 in cancer cells most likely leads to hypermethylation and shutdown of *TIMP2* and *TIMP3* genes.

Exciting evidence has indicated that TET1 plays an important role in the suppression of global DNA methylation, maintenance

(D) TET1 depletion diminishes TIMP2 and TIMP3 activities. The medium collected from MDA-MB-231 cells with or without *TET1* shRNA was analyzed by reverse zymography assays (see Experimental Procedures). The relative intensity of gelatin in TIMP2 and TIMP3 positions was quantified with ImageJ (right).

(E) TET1 knockdown increases MMP activity. The MMP activity of MDA-MB-231 cells with or without *TET1* shRNA was analyzed by generic fluorogenic assay, quantified and shown as in (D).

Data in (A), (D), and (E) are shown with mean ± SD from triplicate experiments. p values were measured by Student's t test in (B–E). *$p < 0.05$; **$p < 0.01$; ***$p < 0.001$.

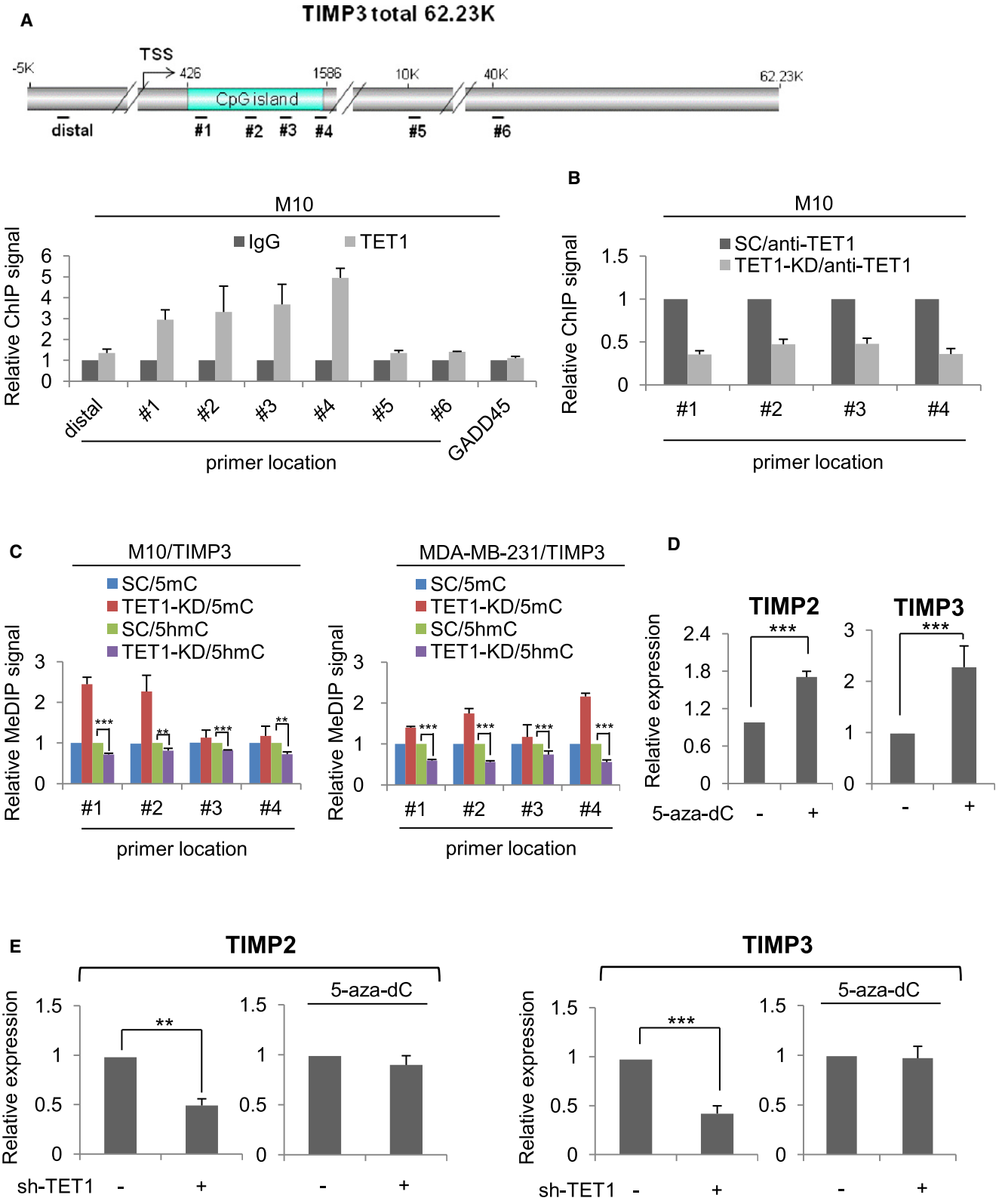

Figure 7. TET1 Binds to *TIMP3* and Inhibits Its Methylation

(A) Endogenous TET1 binds to the CpG island of *TIMP3*. M10 cells were subjected to ChIP with PCR primers (distal, #1, #2, #3, #4, #5, and #6) against the indicated regions along *TIMP3* shown in the diagram above the bar charts. TSS, transcription start site.

of mouse embryonic stem cell state (Ficz et al., 2011; Ito et al., 2010; Tahiliani et al., 2009; Wu et al., 2011), and mouse neuronal activity (Guo et al., 2011). Here, we further provide the first mechanistic evidence demonstrating that TET1 acts as a cancer-invasion suppressor by inhibiting essential downstream gene methylation. In summary, our data indicate that TET1 potentiates *TIMP2* and *TIMP3* expression, which in turn downregulates the MMP activity required for cell invasion. It is likely that during or prior to cancer development, TET1 expression is downregulated. Consequently, TIMP2 and TIMP3 levels are reduced and MMPs are activated, followed by cell invasion and metastasis. Recent findings point out that the TIMP family proteins may have MMP-independent functions in inhibiting cancer formation (Murphy, 2011). Therefore, TET1-mediated TIMP2 and TIMP3 expression may have a broader impact on cancer progression. Our work also highlights and provides detailed data of the two described activities of TET1, its enzymatic activity and DNA-binding capability, in TET1-mediated invasion suppression. In addition, we test our hypothesis that TET1 is an invasion suppressor not only in vitro but also in vivo, correlating TET1 expression levels with xenograft tumor formation and patient outcome. Interestingly, we found that TET1 depletion, in addition to stimulating cell invasion, promoted prostate cancer cell proliferation and migration (Figures 2A and S3). In contrast, knocking down TET1 decreased normal and cancerous breast cell growth and migration (Figures S5D and S5E) but enhanced their invasion ability (Figure 3) in the monolayer cell culture system. These results indicate that TET1 most likely has a differential function in suppressing cancer formation of different origins. The common step regulated by TET1 in both prostate and breast cancers is "cell invasion".

Consistent with our results, several recent reports show a profound loss of *TET* gene expression and/or 5hmC in cancer cell lines (Song et al., 2011) as well as in a variety of human cancers such as breast, prostate, liver, lung, pancreatic, colorectal, gastric, small intestine, brain, kidney, and skin cancers (Haffner et al., 2011; Jin et al., 2011; Kudo et al., 2012; Yang et al., 2012). Indeed, loss of gene expression is not the only way to compromise TET1 function in tumors. *IDH1* and *IDH2* mutations in glioma are found to generate oncometabolite 2-hydroxyglutarate, a known competitive inhibitor of the 2-ketoglutarate-dependent enzymes such as TET proteins (Xu et al., 2011a). Together, these studies and ours strongly suggest that loss of TET1-mediated invasion suppression is most likely universal among human cancers. Additional studies using the recently reported Tet1-deficient mice (Dawlaty et al., 2011) will be useful in providing more decisive in vivo evidence in this regard.

EXPERIMENTAL PROCEDURES

Prostate Cancer Samples and Immunohistochemistry

A total of 153 transurethral resection or prostatectomy specimens of prostate cancer, which received detailed pathological assessment and regular follow-up at the National Taiwan University Hospital, were selected for this study. The study was conducted according to the regulation of the ethics committee, and the specimens were anonymous and analyzed in a blinded manner. For immunohistochemistry, the formalin-fixed, paraffin-embedded tissue sections were deparaffinized and hydrated in a series of graded alcohol to water. Antigen retrieval was performed by incubation of the tissue sections with citrate buffer (DakoCytomation) at 125°C for 5 min. Endogenous peroxidase activity was quenched with 3% H_2O_2 and endogenous biotin was blocked with Background Buster (Innovex Biosciences). Tissue sections were then incubated with TET1 Ab (GeneTex 124207) diluted to a concentration of 1:1000 for 1 hr at room temperature and detected with the STAT-Q IHC staining system (Innovex Biosciences). After development with the substrate 3,3' Diaminobenzidine, the slides were counterstained and mounted for light microscopy analysis.

Cell Migration and Invasion

Migration and invasion were measured with the Real-Time Cell Analyzer (RTCA) Dual Plate (DP) system (xCELLigence, Roche Diagnostics GmbH) and indicated by the cell index as defined in http://www.roche-applied-science.com/sis/xcelligence/index.jsp?&id=xcect_010100. The system monitors cell status using proprietary microelectronic sensor technology. In brief, 2×10^4 to 5×10^4 of cells were seeded with serum-free medium onto the upper chambers of the cellular invasion/migration (CIM) plates. These chambers were then placed on the lower parts of the CIM device, which contained growth medium supplemented with 10% FBS as an attractant. As for invasion, upper chambers were coated with 20 μg of matrigel (BD Biosciences, Cat No. 354234) for 4 hr before cells were added. Cell invasion and migration were monitored every 15 min for 48 hr.

Animal Experiments

Athymic (nu/nu) nude mice and BALB/c mice (6–7 weeks of age) were obtained from the National Laboratory Animal Center and housed as described previously (Tsai et al., 2009). All animal work was performed in accordance with the protocols approved by the Institutional Animal Care and Use Committee, Academia Sinica. For orthotopic implantation of human prostate cancer cells, a nude mouse prostate was exposed with a surgical incision and a suspension of prostate cancer cells (3×10^5 in 20 μl PBS) was injected into the left side of prostate. For breast xenograft tumor experiments, mouse mammary carcinoma 4T1 cells were orthotopically implanted into the fat pad of BALB/c mice. Bioluminescence intensity of implanted tumors was monitored and body weight measured in living mice weekly. Mice were euthanized and necropsied at the end of experiments. A portion of each tumor was snap-frozen in liquid nitrogen and stored at −80°C until needed for western blot analysis of relevant biomarkers. The remainder was fixed in 10% formalin overnight. For the acquisition of prostate cancer cells at different stages, tumors were harvested at 2 weeks or 15 weeks after implantation from prostate and lung tissues.

(B) Controls for TET1 Ab used in the ChIP assays shown in (A). ChIP assays similar to (A) were performed in M10 cells with scramble shRNA (black bars) or *TET1* shRNA (gray bars).

(C) TET1 knockdown increases and decreases *TIMP3* promoter-specific 5mC and 5hmC levels, respectively. M10 or MDA-MB-231 cells with or without *TET1* shRNA were subjected to MeDIP analysis with 5mC or 5hmC Ab. PCR was carried out with four independent pairs of primers with the relative positions indicated in (A). Antibodies used are Flag Ab (a kind gift from Dr. S.C. Lee), TET1 Ab (GeneTex, #124207), IgG (Abcam), 5mC Ab (Eurogentec, BI-MECY-0100), and 5hmC Ab (Active Motif, #39769).

(D) 5-aza-dC derepresses the expression of *TIMP2* and *TIMP3*.

(E) TET1-depletion-mediated repression of *TIMP2* and *TIMP3* is lost in the presence of 5-aza-dC.

(D and E) MDA-MB-231 cells without (D) or with (E) *TET1* shRNA or scramble shRNA were mock treated or treated with 5-aza-dC, followed by real-time RT-PCR analysis of *TIMP2* and *TIMP3* gene expression. In (C–E), p values were measured by Student's t test. $^{**}p < 0.01$; $^{***}p < 0.001$. In (A–E), data are shown as mean ± SD from triplicate experiments.

Human Breast Cancer Specimens

All breast tissue specimens are from the BioBank of the Tri-Service General Hospital. All patients gave informed consent for participation, and the study was approved by the institutional review board of the Tri-Service General Hospital. These patients include individuals with carcinoma in situ and invasive ductal carcinoma of the breast who are undergoing mastectomy and axillary lymph node dissection. Stage was determined according to the AJCC system (American Joint Committee on Cancer, http://www.cancerstaging.org/). All specimens, including cancerous parts and adjacent normal parts, were collected during operations and subsequently stored in liquid nitrogen.

Reverse Zymography and MMP Assays

A total of 5 × 10^5 of MDA-MB-231 cells were seeded onto 6-well plate. After 24 hr, the cells were washed and incubated with serum-free medium for 48 hr. The medium (defined as conditioned medium, CM), was then collected and centrifuged at 1000 × *g* for 10 min, followed by zymography assays (Clark et al., 2010). In brief, CM was mixed with nonreducing 5× sample buffer without boiling and was loaded onto 15% SDS-PAGE containing 0.1% gelatin and serum-free medium after being cultured with M10 cells. Electrophoresis was performed at 125 V for 120 min. The gel was then removed and rinsed twice in enzyme-renaturing buffer (2.5% of Triton X-100, 50 mM Tris-base, 200 mM NaCl, 5 μM ZnCl, 25 mM $CaCl_2$ [pH 7.5]) for 30 min with gentle agitation at room temperature (RT), followed by incubation in the developing buffer (50 mM Tris-base, 200 mM NaCl, 5 μM ZnCl, 25 mM $CaCl_2$ [pH 7.5]) for 30 min with gentle agitation at RT and again in the same buffer for 16–18 hr at 37°C. After being washed three times with deionized water, the gel was stained by coomassie blue staining. Quantification was performed with ImageJ as described previously (Hu and Beeton, 2010). For MMP assays, a SenoLyte 520 Generic MMP Assay Kit (AnaSpec) was used according to the instructions provided by the manufacturer. In brief, CM was mixed with an equal volume of MMP substrate solution in the 96-well black microplate and incubated for 1 hr at RT. The fluorescence intensity was measured by a Victor 3 1420 multilabel counter (Perkin Elmer) at Ex/Em = 540 nm/575 nm.

Chromatin Immunoprecipitation

Chromatin immunoprecipitation assays were performed as described previously (Hsu et al., 2004) except that the eluted DNA was extracted via a PCR purification kit (QIAGEN). DNA was then analyzed by real-time qPCR (LightCycler 480, Roche). The amplifications were performed in a reaction volume of 20 μl containing 2 μl of immunoprecipitated material. The sequences of DNA primers for ChIP are listed in the Extended Experimental Procedures.

Methylated DNA Immunoprecipitation

Genomic DNA was prepared with a genomic DNA extraction kit (QIAGEN, #51304) and sonicated with Bioruptor (Diagenode) to produce random fragments ranging in mean size from 300 to 1,000 bp. 5 μg of fragmented DNA was denatured for 10 min at 95°C and immunoprecipitated overnight at 4°C with 5 μl of 5-methylcytidine antibody (Eurogentec) in a final volume of 500 μl IP buffer (10 mM sodium phosphate [pH 7.0], 140 mM NaCl, 0.05% Triton X-100). The mixture was incubated with 30 μl magnetic beads (Milipore) for another 4 hr at 4°C and washed three times with 1 ml of IP buffer. Beads were resuspended with 250 μl digestion buffer (50 mM Tris [pH 8.0], 10 mM EDTA, 0.5% SDS) containing 5 μl proteinase K (20 mg/ml stock) and shaken overnight at 56°C. DNA was extracted with a QIAGEN Kit (QIAGEN, #28106) and analyzed by real-time PCR.

5-aza-dC Treatment

The demethylation agent 5-aza-dC was added to the culture medium at the concentration of 10 μM. Cells were harvested and RNAs analyzed by quantitative real-time RT-PCR 5 days after 5-aza-dC treatment.

For other methods, please see the Extended Experimental Procedures.

SUPPLEMENTAL INFORMATION

Supplemental Information includes Extended Experimental Procedures and 14 figures and can be found with this article online at http://dx.doi.org/10.1016/j.celrep.2012.08.030.

LICENSING INFORMATION

ACKNOWLEDGMENTS

We thank Drs. W.H. Lee at UCI and Y. Zhang at UNC for critical suggestions, S.C. Lee at NTU for providing the Flag antibody, and Y.C. Chang at NTUH for helping with statistics and analyzing patient survival. We also thank the National RNAi Core Facility at Academia Sinica for providing shRNA constructs and Affymetrix Gene Expression Service Laboratory at Academia Sinica for performing the microarray experiments. This research was primarily supported by a career development grant from Academia Sinica to L.-J.J. and partially supported by National Science Council grants to P.-W.H. (NSC 98-2320-B-001-018-MY) and H.-D.H. (NSC-100-2911-I-009-101).

Received: May 12, 2012
Revised: July 12, 2012
Accepted: August 31, 2012
Published online: September 20, 2012

REFERENCES

An, W., Kim, J., and Roeder, R.G. (2004). Ordered cooperative functions of PRMT1, p300, and CARM1 in transcriptional activation by p53. Cell *117*, 735–748.

Anania, M.C., Sensi, M., Radaelli, E., Miranda, C., Vizioli, M.G., Pagliardini, S., Favini, E., Cleris, L., Supino, R., Formelli, F., et al. (2011). TIMP3 regulates migration, invasion and in vivo tumorigenicity of thyroid tumor cells. Oncogene *30*, 3011–3023.

Bachman, K.E., Herman, J.G., Corn, P.G., Merlo, A., Costello, J.F., Cavenee, W.K., Baylin, S.B., and Graff, J.R. (1999). Methylation-associated silencing of the tissue inhibitor of metalloproteinase-3 gene suggest a suppressor role in kidney, brain, and other human cancers. Cancer Res. *59*, 798–802.

Bourboulia, D., and Stetler-Stevenson, W.G. (2010). Matrix metalloproteinases (MMPs) and tissue inhibitors of metalloproteinases (TIMPs): Positive and negative regulators in tumor cell adhesion. Semin. Cancer Biol. *20*, 161–168.

Cameron, E.E., Bachman, K.E., Myöhänen, S., Herman, J.G., and Baylin, S.B. (1999). Synergy of demethylation and histone deacetylase inhibition in the re-expression of genes silenced in cancer. Nat. Genet. *21*, 103–107.

Chernov, A.V., Sounni, N.E., Remacle, A.G., and Strongin, A.Y. (2009). Epigenetic control of the invasion-promoting MT1-MMP/MMP-2/TIMP-2 axis in cancer cells. J. Biol. Chem. *284*, 12727–12734.

Clark, I.M., Swingler, T.E., Sampieri, C.L., and Edwards, D.R. (2008). The regulation of matrix metalloproteinases and their inhibitors. Int. J. Biochem. Cell Biol. *40*, 1362–1378.

Clark, I.M., Young, D.A., and Rowan, A.D. (2010). Matrix metalloproteinase protocols, Second Edition (New York, N.Y.: Humana Press).

Dawlaty, M.M., Ganz, K., Powell, B.E., Hu, Y.C., Markoulaki, S., Cheng, A.W., Gao, Q., Kim, J., Choi, S.W., Page, D.C., and Jaenisch, R. (2011). Tet1 is dispensable for maintaining pluripotency and its loss is compatible with embryonic and postnatal development. Cell Stem Cell *9*, 166–175.

Dawson, M.A., and Kouzarides, T. (2012). Cancer epigenetics: from mechanism to therapy. Cell *150*, 12–27.

Deryugina, E.I., and Quigley, J.P. (2006). Matrix metalloproteinases and tumor metastasis. Cancer Metastasis Rev. *25*, 9–34.

Ficz, G., Branco, M.R., Seisenberger, S., Santos, F., Krueger, F., Hore, T.A., Marques, C.J., Andrews, S., and Reik, W. (2011). Dynamic regulation of 5-hydroxymethylcytosine in mouse ES cells and during differentiation. Nature *473*, 398–402.

Frauer, C., Rottach, A., Meilinger, D., Bultmann, S., Fellinger, K., Hasenöder, S., Wang, M., Qin, W., Söding, J., Spada, F., and Leonhardt, H. (2011). Different binding properties and function of CXXC zinc finger domains in Dnmt1 and Tet1. PLoS ONE *6*, e16627.

Friedl, P., and Alexander, S. (2011). Cancer invasion and the microenvironment: plasticity and reciprocity. Cell *147*, 992–1009.

Guo, J.U., Su, Y., Zhong, C., Ming, G.L., and Song, H. (2011). Hydroxylation of 5-methylcytosine by TET1 promotes active DNA demethylation in the adult brain. Cell *145*, 423–434.

Haffner, M.C., Chaux, A., Meeker, A.K., Esopi, D., Gerber, J., Pellakuru, L.G., Toubaji, A., Argani, P., Iacobuzio-Donahue, C., Nelson, W.G., et al. (2011). Global 5-hydroxymethylcytosine content is significantly reduced in tissue stem/progenitor cell compartments and in human cancers. Oncotarget *2*, 627–637.

He, Y.-F., Li, B.-Z., Li, Z., Liu, P., Wang, Y., Tang, Q., Ding, J., Jia, Y., Chen, Z., Li, L., et al. (2011). Tet-mediated formation of 5-carboxylcytosine and its excision by TDG in mammalian DNA. Science *333*, 1303–1307.

Hojilla, C.V., Wood, G.A., and Khokha, R. (2008). Inflammation and breast cancer: metalloproteinases as common effectors of inflammation and extracellular matrix breakdown in breast cancer. Breast Cancer Res. *10*, 205.

Hsu, C.-H., Chang, M.D.T., Tai, K.-Y., Yang, Y.-T., Wang, P.-S., Chen, C.-J., Wang, Y.-H., Lee, S.-C., Wu, C.-W., and Juan, L.-J. (2004). HCMV IE2-mediated inhibition of HAT activity downregulates p53 function. EMBO J. *23*, 2269–2280.

Hu, X., and Beeton, C. (2010). Detection of functional matrix metalloproteinases by zymography. J. Vis. Exp. *45*, e2445.

Hua, H., Li, M., Luo, T., Yin, Y., and Jiang, Y. (2011). Matrix metalloproteinases in tumorigenesis: an evolving paradigm. Cell. Mol. Life Sci. *68*, 3853–3868.

Ito, S., D'Alessio, A.C., Taranova, O.V., Hong, K., Sowers, L.C., and Zhang, Y. (2010). Role of Tet proteins in 5mC to 5hmC conversion, ES-cell self-renewal and inner cell mass specification. Nature *466*, 1129–1133.

Ito, S., Shen, L., Dai, Q., Wu, S.C., Collins, L.B., Swenberg, J.A., He, C., and Zhang, Y. (2011). Tet proteins can convert 5-methylcytosine to 5-formylcytosine and 5-carboxylcytosine. Science *333*, 1300–1303.

Jin, S.G., Jiang, Y., Qiu, R., Rauch, T.A., Wang, Y., Schackert, G., Krex, D., Lu, Q., and Pfeifer, G.P. (2011). 5-Hydroxymethylcytosine is strongly depleted in human cancers but its levels do not correlate with IDH1 mutations. Cancer Res. *71*, 7360–7365.

Kessenbrock, K., Plaks, V., and Werb, Z. (2010). Matrix metalloproteinases: regulators of the tumor microenvironment. Cell *141*, 52–67.

Ko, M., Huang, Y., Jankowska, A.M., Pape, U.J., Tahiliani, M., Bandukwala, H.S., An, J., Lamperti, E.D., Koh, K.P., Ganetzky, R., et al. (2010). Impaired hydroxylation of 5-methylcytosine in myeloid cancers with mutant TET2. Nature *468*, 839–843.

Kudo, Y., Tateishi, K., Yamamoto, K., Yamamoto, S., Asaoka, Y., Ijichi, H., Nagae, G., Yoshida, H., Aburatani, H., and Koike, K. (2012). Loss of 5-hydroxymethylcytosine is accompanied with malignant cellular transformation. Cancer Sci. *103*, 670–676.

Kulis, M., and Esteller, M. (2010). DNA Methylation and Cancer. In Advances in Genetics, H. Zdenko and U. Toshikazu, eds. (Academic Press), pp. 27–56.

Lorsbach, R.B., Moore, J., Mathew, S., Raimondi, S.C., Mukatira, S.T., and Downing, J.R. (2003). TET1, a member of a novel protein family, is fused to MLL in acute myeloid leukemia containing the t(10;11)(q22;q23). Leukemia *17*, 637–641.

Murphy, G. (2011). Tissue inhibitors of metalloproteinases. Genome Biol. *12*, 233.

Ono, R., Taki, T., Taketani, T., Taniwaki, M., Kobayashi, H., and Hayashi, Y. (2002). LCX, leukemia-associated protein with a CXXC domain, is fused to MLL in acute myeloid leukemia with trilineage dysplasia having t(10;11)(q22;q23). Cancer Res. *62*, 4075–4080.

Smith, E., De Young, N.J., Tian, Z.Q., Caruso, M., Ruszkiewicz, A.R., Liu, J.F., Jamieson, G.G., and Drew, P.A. (2008). Methylation of TIMP3 in esophageal squamous cell carcinoma. World J. Gastroenterol. *14*, 203–210.

Song, C.-X., Szulwach, K.E., Fu, Y., Dai, Q., Yi, C., Li, X., Li, Y., Chen, C.-H., Zhang, W., Jian, X., et al. (2011). Selective chemical labeling reveals the genome-wide distribution of 5-hydroxymethylcytosine. Nat. Biotechnol. *29*, 68–72.

Taberlay, P.C., and Jones, P.A. (2011). DNA methylation and cancer. Prog. Drug Res. *67*, 1–23.

Tahiliani, M., Koh, K.P., Shen, Y., Pastor, W.A., Bandukwala, H., Brudno, Y., Agarwal, S., Iyer, L.M., Liu, D.R., Aravind, L., and Rao, A. (2009). Conversion of 5-methylcytosine to 5-hydroxymethylcytosine in mammalian DNA by MLL partner TET1. Science *324*, 930–935.

Tsai, C.-H., Lin, F.-M., Yang, Y.-C., Lee, M.-T., Cha, T.-L., Wu, G.-J., Hsieh, S.-C., and Hsiao, P.-W. (2009). Herbal extract of Wedelia chinensis attenuates androgen receptor activity and orthotopic growth of prostate cancer in nude mice. Clin. Cancer Res. *15*, 5435–5444.

Williams, K., Christensen, J., Pedersen, M.T., Johansen, J.V., Cloos, P.A.C., Rappsilber, J., and Helin, K. (2011). TET1 and hydroxymethylcytosine in transcription and DNA methylation fidelity. Nature *473*, 343–348.

Wu, S.C., and Zhang, Y. (2010). Active DNA demethylation: many roads lead to Rome. Nat. Rev. Mol. Cell Biol. *11*, 607–620.

Wu, H., and Zhang, Y. (2011a). Mechanisms and functions of Tet protein-mediated 5-methylcytosine oxidation. Genes Dev. *25*, 2436–2452.

Wu, H., and Zhang, Y. (2011b). Tet1 and 5-hydroxymethylation: a genome-wide view in mouse embryonic stem cells. Cell Cycle *10*, 2428–2436.

Wu, H., D'Alessio, A.C., Ito, S., Xia, K., Wang, Z., Cui, K., Zhao, K., Sun, Y.E., and Zhang, Y. (2011). Dual functions of Tet1 in transcriptional regulation in mouse embryonic stem cells. Nature *473*, 389–393.

Xu, W., Yang, H., Liu, Y., Yang, Y., Wang, P., Kim, S.-H., Ito, S., Yang, C., Wang, P., Xiao, M.-T., et al. (2011a). Oncometabolite 2-hydroxyglutarate is a competitive inhibitor of α-ketoglutarate-dependent dioxygenases. Cancer Cell *19*, 17–30.

Xu, Y., Wu, F., Tan, L., Kong, L., Xiong, L., Deng, J., Barbera, A.J., Zheng, L., Zhang, H., Huang, S., et al. (2011b). Genome-wide regulation of 5hmC, 5mC, and gene expression by Tet1 hydroxylase in mouse embryonic stem cells. Mol. Cell *42*, 451–464.

Yang, H., Liu, Y., Bai, F., Zhang, J.Y., Ma, S.H., Liu, J., Xu, Z.D., Zhu, H.G., Ling, Z.Q., Ye, D., et al. (2012). Tumor development is associated with decrease of TET gene expression and 5-methylcytosine hydroxylation. Oncogene. Published online March 5, 2012. http://dx.doi.org/10.1038/onc.2012.67.

You, J.S., and Jones, P.A. (2012). Cancer genetics and epigenetics: two sides of the same coin? Cancer Cell *22*, 9–20.

Zeng, Z.-S., Cohen, A.M., and Guillem, J.G. (1999). Loss of basement membrane type IV collagen is associated with increased expression of metalloproteinases 2 and 9 (MMP-2 and MMP-9) during human colorectal tumorigenesis. Carcinogenesis *20*, 749–755.

Zhang, H., Zhang, X., Clark, E., Mulcahey, M., Huang, S., and Shi, Y.G. (2010). TET1 is a DNA-binding protein that modulates DNA methylation and gene transcription via hydroxylation of 5-methylcytosine. Cell Res. *20*, 1390–1393.